Available online at www.sciencedirect.com
ScienceDirect
International Journal of Thermal Sciences 48 (2009) 708–721
International Journal of Thermal Sciences
www.elsevier.com/locate/ijts

Unsteady numerical simulation of the cooling process of vertical storage tanks under laminar natural convection

I. Rodríguez, J. Castro, C.D. Pérez-Segarra, A. Oliva *

Heat and Mass Transfer Technological Center (CTTC), Polytechnical University of Catalonia (UPC), Colom 11, 08222 Terrassa, Barcelona, Spain

Received 25 February 2008; received in revised form 27 May 2008; accepted 8 June 2008

Available online 14 July 2008

Abstract

The transient cooling of a fluid initially at rest inside a vertical cylinder submitted to heat losses through the walls is studied. The study is restricted to laminar flow conditions. In order to identify the relevant non-dimensional groups that define the unsteady natural convection phenomenon that occurs, a non-dimensional analysis is carried out. The long-term behaviour of the fluid is modelled by formulating a prediction model based on global balances. A parametric study by means of several multidimensional numerical simulations led to correlate the Nusselt number and the transient mean fluid temperature, in order to feed the global model proposed. Special attention is given to the appropriateness of the spatial and time discretisation adopted, the verification of the numerical solutions and the post-processing tasks carried out in order to obtain the correlations. The most relevant particularities of the numerical model developed are also pointed out.

Keywords: Unsteady natural convection; CFD simulations; Storage tanks

1. Introduction

The performance of thermal energy storage tanks is significantly affected by the natural convection and associated heat transfer during charging and discharging phases, but also during their static mode of operation, where the heat exchange with the surroundings is the main mechanism of fluid movement inside the tank. Thus, an effective optimisation of these devices requires an extensive knowledge of the heat transfer mechanism between the fluid and the environment.

Due to its importance for many practical applications such as HVAC, thermal energy storage, among others; the transient process of cooling (or heating) a fluid inside an enclosure under natural convection, has been widely treated in the literature. However, most of the studies conducted have been focused on rectangular enclosures with imposed vertical wall temperatures on steady state situations [1–4] or considering the transient response of the fluid [5–7].

On the other hand, cylindrical geometries have received less attention. Among the earlier studies, the work conducted by Hyun [8] can be cited. He studied the transient mechanism of heat-up a fluid inside a cylinder initially at rest, submitted to a linear temperature gradient at the side wall. Raithby and Hollands [9] in their review cited the experimental studies carried out by Evans and Stefany about the transient response of fluids inside vertical and horizontal enclosures following a step change in wall temperature. These authors correlated the empirical data obtained in the quasi-steady regime to a single expression of the Nusselt number as a function of the Rayleigh number. Cotter and Charles [10,11], in two papers, studied the transient natural convection of crude oil in a large vertical cylinder, presenting results of the time dependence of the Nusselt number and fluid temperature for several oil viscosities and aspect ratios.

More recently, Lin and Armfield [12] studied the transient response of the fluid in a vertical cylinder after a step change in the temperature wall until the stratification stage is reached. After this study, these authors [13] analysed the long-term behaviour of the cooling process in a vertical cylinder with fixed walls temperatures.

* Corresponding author. Tel.: +34 93 739 8192; fax: +34 93 739 8101.
E-mail address: cttc@cttc.upc.edu (A. Oliva).
URL: http://wwww.cttc.upc.edu (A. Oliva).

1290-0729/$ – see front matter
doi:10.1016/j.ijthermalsci.2008.06.002

Nomenclature

c_p	specific heat at constant pressure	$J\,kg^{-1}\,K^{-1}$	
D	tank internal diameter	m	
Gr	Grashof number, $Gr = g\beta\Delta T L_{ref} L_{ref}^3/\nu^2$		
H	tank internal height	m	
$\overline{h}$	fluid global superficial heat transfer coefficient	$W\,m^{-2}\,K^{-1}$	
h_{ext}	external superficial heat transfer coefficient	$W\,m^{-2}\,K^{-1}$	
k	thermal conductivity	$W\,m^{-1}\,K^{-1}$	
L_{ref}	reference length	m	
$\overline{Nu}$	average Nusselt number, Eq. (14)		
n_r	number of control volumes in radial direction		
n_z	number of control volumes in axial direction		
Pr	Prandtl number, $Pr = \nu/\alpha$		
p_d	dynamic pressure	Pa	
p_d^*	non-dimensional dynamic pressure, $p^* = p_d/\rho v_{ref}^2$		
$\dot{Q}_{loss}$	instantaneous heat losses	W	
$\vec{q}$	heat flux vector	$W\,m^{-2}$	
Ra	Rayleigh number, $Ra = g\beta\Delta T_{ref} L_{ref}^3/\nu\alpha$		
r^*	non-dimensional radial distance, $r^* = r/L_{ref}$		
S	inner area of the tank	m^2	
T_0	initial temperature	K	
T	fluid temperature	K	
$\overline{T}$	mean fluid temperature	K	
$\overline{T}_w$	mean wall temperature	K	
T_{env}	ambient temperature	K	
T_{ref}	reference temperature, $T_{ref} = (T_0 + T_{env})/2$	K	
ΔT_{ref}	reference temperature difference, $\Delta T_{ref} = T_0 - T_{env}$	K	
t	time	s	
Δt	time increment	s	
$\overline{U}$	overall heat transfer coefficient	$W\,m^{-2}\,K^{-1}$	
$\widehat{U}$	non-dimensional overall heat transfer coefficient, $\widehat{U} = \overline{U}H/k$		
$\vec{v}$	velocity vector	$m\,s^{-1}$	
$\vec{v}^*$	non-dimensional velocity vector, $\vec{v}^* = \vec{v}/v_{ref}$		
v_{ref}	reference velocity, $v_{ref} = \alpha/L_{ref}$	$m\,s^{-1}$	
z^*	non-dimensional z-coordinate, $z^* = z/L_{ref}$		

Greek letters

α	thermal diffusivity	$m^2\,s^{-1}$
δ_{ins}	insulation thickness	m
δ_t	wall thickness	m
ϵ	relative error	%
ν	kinematic viscosity	$m^2\,s^{-1}$
$\partial\Omega$	surface which enclosed the volume Ω	m^2
ρ	density	$kg\,m^{-3}$
τ	non-dimensional time, $\tau = t v_{ref}/L_{ref}$	
Θ	non-dimensional temperature, $\Theta = (T - T_{env})/\Delta T_{ref}$	
Ω	volume	m^3

Oliveski et al. [14] investigated the cooling of a vertical storage tank considering both the tank and insulation material. They considered different aspect ratios, insulation thicknesses for two different tank volumes and correlated the Nusselt number to the aspect ratio, the mean fluid temperature and the overall heat transfer coefficient for each tank volume studied. Although the correlations obtained by [14] can be very useful, it is difficult to extrapolate their results to other situations than those exposed in their work. The lack of a non-dimensional analysis together with the fact that the correlations proposed were written as a function of dimensional parameters limit their range of application to the specific cases studied.

Papanicolaou and Belessiotis [15] analysed numerically the natural convection in a vertical cylinder with an imposed constant heat flux in its lateral surface. They considered laminar and turbulent regimes, also comparing their numerical results for the transient temperature in the core of the cylinder with an analytical expression given in the literature. Recently, Fernandez-Seara et al. [16] carried out experimental tests to study the static heating and cooling periods of an electrical hot water storage tank, characterising its thermal performance and degree of stratification.

The study of the unsteady behaviour of the fluid is not only of interest as a heat transfer and fluid dynamic problem, but also as a practical situation. For example, in the long-term analysis of solar domestic hot water systems, storage tanks play an active role, as they are an active part of those systems, whose thermal performance is affected by the transient response of the tank. Furthermore, the static mode of operation in such systems, can represent in some cases more than 12 h per day, being an important fraction of the time in long-term operation of solar installations.

Considering this and the scarce information available in the literature on this phenomena, the aim of this work is to investigate by means of numerical CFD simulations, the unsteady natural convection inside a vertical storage tank submitted to heat losses to the environment through top, bottom and lateral walls. The behaviour of the fluid has been characterised and a global model has been presented. In order to obtain the main coefficients needed for these kinds of global models, a non-dimensional analysis has been performed. From this analysis, the relevant non-dimensional groups that define the problem have been identified. A scaling relation to correlate the non-dimensional heat transfer coefficient to the relevant parameters has been proposed. As far as the authors know, there are no available correlations in the literature, such as those proposed, for evaluating the transient heat transfer coefficient inside cylindrical cavities in order to characterise heat losses through the top, bottom and lateral composite walls. In addition, the parametric study carried out has been selected in order to cover a wide range of working conditions for small storage tanks used in domestic hot water systems.

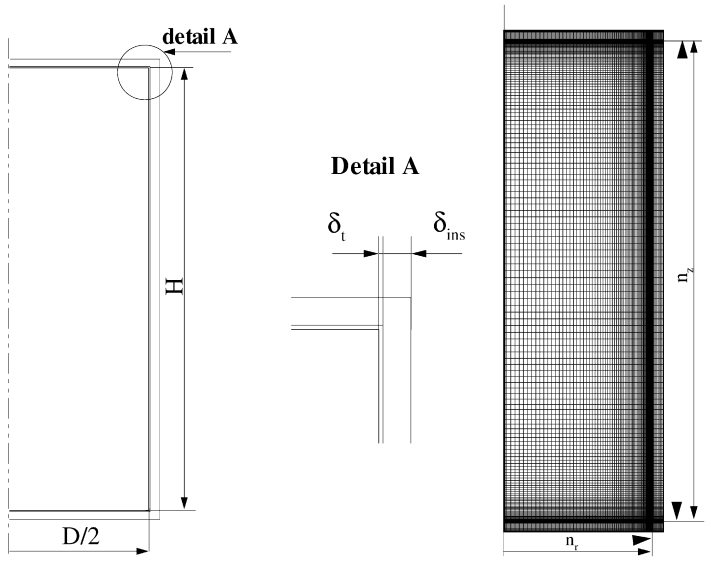

Fig. 1. (a) Scheme of the geometry of the storage tank under study. (b) Computational domain.

2. Problem definition

In an attempt to investigate the transient phenomena that takes place during the cooling-down of vertical hot water storage tanks used for solar domestic hot water systems, different parameters and working conditions have been studied. For the parametric study, the working conditions of small storage tanks for domestic hot water applications have been considered. In this range, most used storage tanks have tank volumes up to 0.4 m^3 with aspect ratios within $1.5 \leqslant H/D \leqslant 3.5$.

In this study, composite walls of stainless steel of 3 mm thick and fibre glass thermal insulation thickness varying within the range $0 \leqslant \delta_{ins} \leqslant 0.04$ m have been considered. These values cover most of the aspect ratios and insulation thicknesses used in commercial storage tanks. A scheme of the vertical cylindrical storage tank is shown in Fig. 1(a).

The fluid has experienced a cooling process due to a temperature gradient between the fluid and the ambient. Taking into account that the service water temperature in domestic hot water applications is around 60 °C, initial temperature of the tank, including solid walls and insulation material, has been considered in the range of $40 \leqslant T_0 \leqslant 70$ °C. Ambient temperature has been fixed to $T_{env} = 20$ °C during the whole cooling process.

For the situation under study, it can be considered that there are not significant variations between the external heat transfer coefficient on the lateral and on the top wall. Furthermore, taking into account that most of commercial storage tanks are supported by feet or suspended from the vertical wall, it can also be assumed that the external convection heat transfer coefficient on the bottom wall is the same that on the top and lateral walls. Thus, external heat transfer coefficient on the walls has been set to h_{ext}= 10 W/m^2 K. This value is in correspondence with similar situations described by others authors [10,11,14]. Moreover, aiming a generalisation of the problem, a limiting lower value of $h_{ext} = 2$ W/m^2 K has also been set.

For the specified conditions the flow is assumed laminar. A detailed discussion is given in Section 3.1.

3. Mathematical model, numerical simulation and verification process

In this section the mathematical model used for the numerical simulation of the problem described above is presented. The post-processing tasks carried out in order to select an appropriate spacial and temporal discretisation are also described.

3.1. Mathematical model

The fluid flow and heat transfer phenomena involved in the transient natural convection inside a storage tank is governed by the continuity, momentum and energy conservation equations. Concerning to the fluid regime, there is a lack of information, e.g., critical Rayleigh number, to be used as evidence under realistic situations. However, among the studies carried out under similar working conditions as those described in the previous section, the work conducted by Oliveski et al. [14] can be cited. They studied experimental and numerically the laminar convection in storage tanks submitted to heat losses to the environment. In their study, experimental data were well reproduced by the numerical results obtained. Storage tanks parameters studied (tank volumes, aspect ratios, initial temperature, insulation thickness, etc.) were within the range of parameters considered in the present work. In addition, Papanicolaou and Belessiotis [15], studied the transient heating of a fluid by an imposed heat flux on the sidewall for Rayleigh numbers between $10^{10} \leqslant Ra \leqslant 10^{15}$. They have found that laminar regime can be obtained for Rayleigh numbers up to $Ra = 10^{13}$ while turbulent flow should be expected for $Ra \geqslant 5 \cdot 10^{13}$. Taking into account the range of parameters of the present work and the aforementioned results, the hypothesis of laminar flow has been considered.

In the formulation presented, it has also been assumed a Newtonian fluid behaviour, constant physical properties except density variations in the buoyancy terms of the momentum equations (Boussinesq approximation), viscous dissipation negligible, and non-participant radiating medium. Thus, the governing equations can be written as follows:

$$\nabla \cdot \vec{v} = 0 \tag{1}$$

$$\frac{\partial \vec{v}}{\partial t} + \vec{v} \cdot \nabla \vec{v} = -\frac{1}{\rho}\nabla p_d + \frac{1}{\rho}\nabla \cdot \vec{\tau} - \vec{g}\,\beta(T - T_0) \tag{2}$$

$$\frac{\partial T}{\partial t} + \vec{v} \cdot \nabla T = \alpha \nabla^2 T \tag{3}$$

The computational domain considered includes the fluid inside the storage, the tank walls and the insulation material. In the energy equation, the external ambient temperature and the superficial heat transfer coefficient have been imposed on the vertical, top and bottom walls, neglecting the radiation heat transfer between the tank and the ambient. At $t = 0$, the whole domain has been set to an initial temperature value of $T = T_0$.

3.2. Numerical approach

The governing equations together with the boundary conditions have been integrated over the whole domain (fluid, solid walls and insulation material) by means of finite-volume techniques with fully implicit first order temporal differentiation, using cylindrical staggered grids. Diffusive terms have been evaluated using a second order central differences scheme, while convective terms have been approximated by means of the high order SMART scheme [17] using a deferred correction approach. The SIMPLEC algorithm has been used to solve the coupling between pressure and velocity fields [18]. The algebraic system of linear equations resulting for each variable have been solved by using a Multigrid method [19].

Due to the symmetry of the situation presented in Section 2, the computational domain selected is axisymmetric. Considering the fluid structure and with the objective of describing the boundary layer near the walls (where the temperature and velocity gradients are the largest), it has been necessary to concentrate the mesh at the interface between the fluid and the solid wall by means of a tanh-like distribution. The computational domain for the fluid has been discretised into non-uniform meshes of $n_r \mathrm{x} n_z$ control volumes (CV) with a concentration factor of 2 in the zones near the interface between liquid and solid (i.e. near the tank walls), while for the solid domain (tank wall and insulation material) regular meshes have been used. In Fig. 1(b), the computational grid for one of the cases considered ($H/D = 2$) is shown (mesh concentration near the walls is indicated with black triangles).

Regarding the criteria to stop transient simulation, as the time needed to cool down the fluid inside the tank, i.e. to reach the ambient temperature, it is theoretically infinite, transient simulation have been finished once the mean temperature of the fluid has reached a value of $\bar{\Theta} \leqslant 0.10$. On the other hand, for each time step, the iterative procedure has been truncated once the non-dimensional variables increments and residuals have been lower than $10^{-5}\%$, and once the relative increments of the computed mean Nusselt number has been below $10^{-7}\%$.

Table 1
Definition of the relevant parameters for the verification process

Case	H/D [–]	Ra [–]	$\widehat{U}$ [–]	T_0 [°C]	h_{ext} [W/m^2 K]	δ_{ins} [m]	Ω [m^3]
v1	1	7.132×10^{11}	11.594	60	10	0.02	0.3
v2	2	2.394×10^{12}	5.178	60	10	0.01	0.3
v3	3	5.387×10^{12}	24.23	60	10	0	0.3
v4	3.45	7.142×10^{12}	3.594	60	2	0.01	0.3

3.3. Code and numerical solutions verification

With the objective of obtaining reliable solutions, it is important to submit the code and numerical solutions to a process of verification. The verification of the code accounts for the identification of possible programming errors, while the verification of numerical solutions is concerned with the quantification of errors due to computational sources (spacial and temporal discretisation, convergence, etc.). In the process of code verification, the code used in the numerical simulations has been verified by using different techniques such as to submit the code to different problems with known analytical solutions, comparison with well-known benchmark cases reported in the literature and, also by the Method of Manufactured Solutions (MMS) [20], which is based in generate an analytical solution that exercises all the terms in the governing equations. The main tasks carried out during the process of the verification of the code used in the present work can be found in detail in [21,22].

Regarding to numerical solutions verification, numerical solutions presented have been obtained adopting an *h-refinement* criteria. Fixing numerical schemes, verification of the results account for the influence of the mesh spacing and the time increment on these numerical results. The parametric study carried out in the present work accounts for a determined number of computations. The post-processing verification presented here compresses four of these computations, one for each aspect ratio considered. These cases have been considered representative of all the others. The main parameters of each of these cases are given in Table 1. Notice that together with the non-dimensional relevant groups, the dimensional parameters (insulation thickness, tank volume, initial temperature, external heat transfer coefficient) are also given. These verification cases are hereafter denoted as *case v1*, *case v2*, *case v3* and *case v4*.

For each of these computations, the mesh has been refined using 4 levels on the *h-refinement* criteria with a ratio of 2 (in each computational level, denoted with letter 'm', the mesh has been doubled, see Table 2). The criteria of refinement adopted, considers the fluid and the solid domains independently, as shown in the table. Moreover, the simulation time has also been discretised in time steps of 0.25, 0.5, 1.0 and 2.0 s.

Concerning the temporal discretisation, *case v2* has been selected for the third level of spacial discretisation according to

Table 2
Number of CV in the h-refinement procedure for each aspect ratio including the fluid and solid walls $n_r \times n_z = (n_f + n_t + n_{\text{ins}}) \times (n_f + n_t + n_{\text{ins}})$

	H/D	
	1	2
m_1	$(23+1+2)\times(23+2+4)$	$(18+1+2)\times(36+2+4)$
m_2	$(46+2+4)\times(46+4+8)$	$(36+2+4)\times(72+4+8)$
m_3	$(92+4+8)\times(92+8+16)$	$(72+4+8)\times(144+8+16)$
m_4	$(184+8+16)\times(184+16+32)$	$(144+8+16)\times(288+16+32)$
	H/D	
	3	3.45
m_1	$(16+1+2)\times(48+2+4)$	$(15+1+2)\times(53+2+4)$
m_2	$(32+2+4)\times(96+4+8)$	$(30+2+4)\times(105+4+8)$
m_3	$(64+4+8)\times(192+8+16)$	$(60+4+8)\times(210+8+16)$
m_4	$(128+8+16)\times(384+16+32)$	$(120+8+16)\times(420+16+32)$

Table 2. The case has been solved up to 7200 s using the different time steps indicated above. For time steps of $\Delta t = 1$ s and $\Delta t = 2$ s convergence has been reached after a high number of outer iterations. During the first instants of the cooling process (up to 900 s), the iterative process has required more than 200 iterations for $\Delta t = 1$ s. Furthermore, for the highest time step ($\Delta t = 2$ s) the convergence has been totally unstable, and in most time steps the convergence criteria has not been attained after 300 iterations. Although this number decreases with the development of the fluid stratification, it still has required more than 50 iterations to achieve convergence criteria imposed at each time step. For the smallest Δt, the number of outer iterations required has always been below 20 even for the first instants, being around 8 and 12 for $\Delta t = 0.25$ s and $\Delta t = 0.5$ s, respectively. For the smallest time steps, discrepancies between solutions obtained have not been noticeable. As the time to cool down the storage could be very large, depending on the situation under study, a high number of time increments to solve it is required. Considering the total number of time increments to be solved and the number of outer iterations per each one needed to reach convergence, a temporal discretisation of $\Delta t = 0.5$ s has been adopted.

The influence of the mesh spacing has been analysed by fixing the time step to $\Delta t = 0.5$ s. Thus, simulations have been performed following the *h-refinement* criteria on the four cases selected. These cases have been solved up to 7200 s. In Fig. 2 the temperature profiles near the boundary layer obtained with the different levels of refinement at selected tank heights and two time increments for the *case v3* are shown. As can be seen, there are no noticeable differences between level of refinement m_3 and m_4. In Table 3 comparisons between the different levels of refinement for the average Nusselt number at different time instants are given. For the brevity of the manuscript, all the results obtained for the verification cases are not shown. Thus in the table the results correspond only to *case v2* and *case v4*. In general, all cases exhibit the same trend. Thus, these results have been considered representative of the verification process performed. Major discrepancies have been observed for the first instants, where the formation of the boundary layer takes place. However, relative errors of the variables at the initial instants, between level of refinement $m3$ and $m4$ have been below 1%.

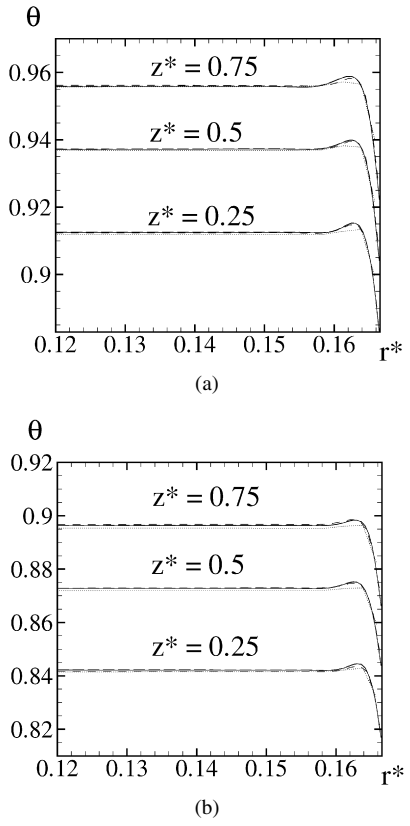

Fig. 2. Fluid temperature profiles at different heights with different levels of refinement for *case v3*: dotted line (m1), dash-dotted line (m2), dashed line (m3), and solid line (m4) (a) at 3600 s and (b) at 7200 s.

Table 3
Verification. Average Nusselt number at different instants. Comparison between levels of refinement

case v2								
	$t = 900$ s		$t = 1800$ s		$t = 3600$ s		$t = 7200$ s	
	$\overline{Nu}$	ϵ [%]	$\overline{Nu}$	ϵ [%]	$\overline{Nu}$	ϵ [%]	$\overline{Nu}$	ϵ [%]
m1	281.864	1.91	268.349	1.10	240.376	1.91	219.482	0.50
m2	293.618	2.20	269.231	1.43	241.881	0.85	220.169	0.81
m3	286.942	0.15	267.884	0.92	243.298	0.68	217.964	0.16
m4	287.373	–	265.428	–	244.956	–	218.393	–
case v4								
	$t = 900$ s		$t = 1800$ s		$t = 3600$ s		$t = 7200$ s	
	$\overline{Nu}$	ϵ [%]	$\overline{Nu}$	ϵ [%]	$\overline{Nu}$	ϵ [%]	$\overline{Nu}$	ϵ [%]
m1	366.679	3.81	368.281	1.93	357.577	2.25	242.082	2.94
m2	378.163	0.79	373.907	0.43	361.461	1.18	330.850	0.43
m3	379.700	0.39	374.117	0.37	363.071	0.74	333.746	0.44
m4	381.184	–	375.520	–	365.789	–	332.299	–

As time goes by, differences between the levels of refinement tend to level out. It has been found that the third level of discretisation (grids denoted as m_3 in Table 2) provides a good compromise between the computational time to simulate the whole cooling process of the tank and the accuracy of the results. Taking into account the analysis performed, the results presented in this work have been obtained with the third level of refinement (m_3).

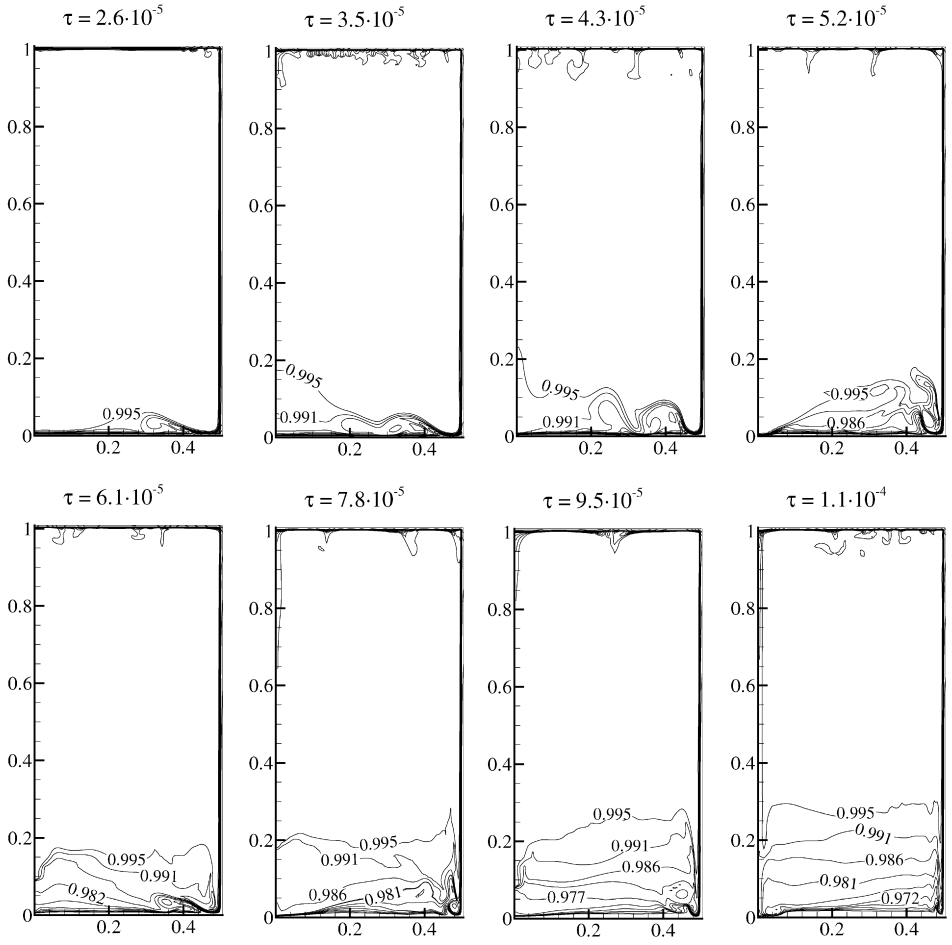

Fig. 3. Transient evolution of the fluid inside the storage tank. Temperature contours. $\tau = 2.6 \cdot 10^{-5}$ to $\tau = 1.1 \cdot 10^{-4}$. $Ra = 5.986 \cdot 10^{11}$, $H/D = 1$, and $U^* = 11.6$.

3.4. Physical analysis of the fluid structure

The transient natural convection phenomena taking place inside the storage tank is illustrated in Figs. 3 to 6. In these figures, the transient evolution of temperature contours and velocity vectors at different instants of the cooling process, for one of the cases analysed, are shown. The case illustrated in the figures is defined by $\Omega = 0.3$ m^3, $T_0 = 60\,^{\circ}$C, $H/D = 1$, $\delta_{\text{ins}} = 0$ m and $h = 10$ W/m^2 K. In all figures, variables are given in non-dimensional form (see definition in nomenclature).

In Fig. 3 it is shown how at the first instants, when the transient convection starts, the thermal boundary layer develops rapidly on the vertical wall ($\tau = 2.6 \cdot 10^{-5}$). The cooled fluid near the wall travels down and moves along the bottom wall forming waves that advance toward the center of the tank. These waves of cooled fluid interact continuously with the fluid in the core. When the perturbation arrives to the center of the tank, it forms an upward crest ($\tau = 3.5 \cdot 10^{-5}$) and then turns back to the vertical wall. At this point, this reverse wave interacts with newly formed waves of cooled fluid descending along the vertical wall ($\tau = 5.2 \cdot 10^{-5}$). This process is well illustrated in Fig. 4, where velocity vectors are shown. In addition, the figure shows how convective cells are continuously formed at the top wall and transported to the core of the tank.

This movement of the cold fluid in the bottom of the tank, back and forth like a wave motion, interacting with the surrounding fluid and the cold stream descending on the sidewall, until it dissipates, continues for just a few instants. The cold stream travelling down and flowing on the bottom, tends to increase its temperature due to the continuous mixing with the fluid in the bottom region. These fluid intrusions evolve into the formation of stratification of the fluid inside the tank (see $\tau = 6.1 \cdot 10^{-5}$ to $\tau = 1.1 \cdot 10^{-4}$ in Figs. 3 and 4). In Fig. 4 it is clearly shown how as the fluid became stratified in the bottom zone, fluid vortices are displaced from the bottom to the central regions.

As the interaction between the cooled fluid on the sidewall and the fluid in the core continues, the stratification of the fluid temperatures advances from the bottom to the top ($\tau = 2.6 \cdot 10^{-4}$ to $\tau = 2.8 \cdot 10^{-3}$). The fluid stagnation region increase its size while the fluid movement is limited to the upper part of the tank (see Fig. 6). As time marches, thermal stratification continues at a progressive reduced rate due to the decreasing of driving buoyancy forces until it approaches to a quasi-steady regime (Fig. 5). Similar quasi-steady regimes have been reported before in the literature [12,15]. However in those studies, the top and bottom walls were considered adiabatic.

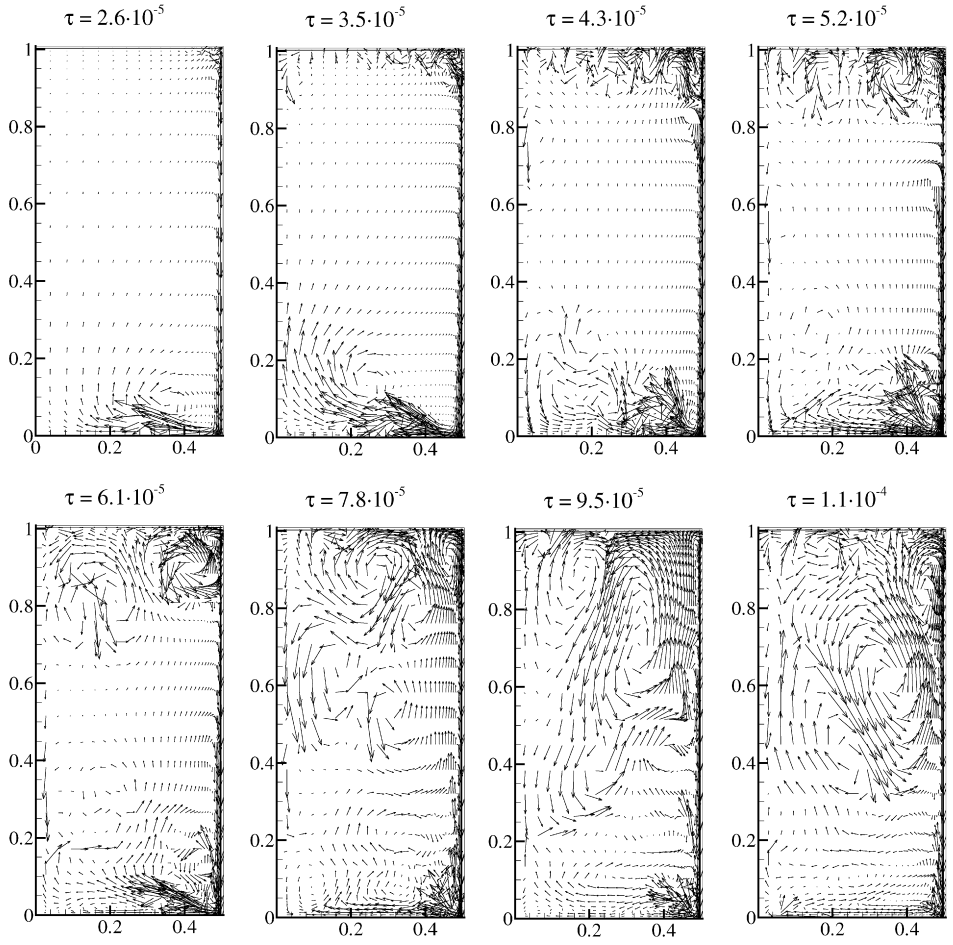

Fig. 4. Transient evolution of the fluid inside the storage tank. Velocity vectors. $\tau = 2.6 \cdot 10^{-5}$ to $\tau = 1.1 \cdot 10^{-4}$. $Ra = 5.986 \cdot 10^{11}$, $H/D = 1$, and $U^* = 11.6$.

For the case illustrated as an example of the transient evolution of the fluid, this transition occurs around $\tau = 2.8 \cdot 10^{-3}$. When the fluid reach the quasi-steady regime, three regions are clearly formed. A region of stratified fluid at most of 25% of the bottom part of the tank with a steep temperature gradient. A mixed region in the upper part of the tank, with 25% of the tank volume approximately and, a wide transition region between the stratified and mixed fluid. The mixed zone in the upper region of the tank was not reported in previous studies, as the bottom and top walls were adiabatic, and heat transfer was taking place only on the vertical wall. In the present study, as the top of the tank is not adiabatic, the heat transfer on the top wall continues during the whole cooling process, promoting the mixing of the fluid in that zone.

The quasi-steady regime remains until the fluid inside the storage is completely cooled ($\tau = 3.1 \cdot 10^{-3}$ to $\tau = 5.2 \cdot 10^{-2}$), representing about 94% of the cooling process.

4. Evaluation of the global heat transfer coefficient

Taking into account the global model presented in the next section (see Section 5), the tasks carried out to obtain the global heat transfer coefficient between the fluid and the inner tank walls are hereafter outlined.

4.1. Non-dimensional analysis

The governing equations have been non-dimensionalised by substituting: $r = L_{\text{ref}} r^*$, $z = L_{\text{ref}} z^*$, $t = L_{\text{ref}}\tau / v_{\text{ref}}$, $\vec{v} = v_{\text{ref}} \vec{v}^*$, $p_d = \rho v_{\text{ref}}^2 p_d^*$ and $T = T_{\text{env}} + \Delta T_{\text{ref}} \Theta$. The characteristic dimension of the body, reference velocity and temperature assumed have been $L_{\text{ref}} = H$, $v_{\text{ref}} = \alpha / L_{\text{ref}}$, $\Delta T_{\text{ref}} = T_0 - T_{\text{env}}$ and $T_{\text{ref}} = (T_0 + T_{\text{env}})/2$. Thus, governing equations in their non-dimensional form can be written as:

$$\nabla \cdot \vec{v}^* = 0 \tag{4}$$

$$\frac{D\vec{v}^*}{D\tau} = -\nabla p_d^* + Pr \nabla^2 \vec{v}^* - RaPr\Theta \tag{5}$$

$$\frac{D\Theta}{D\tau} = \nabla^2 \Theta \tag{6}$$

Considering the symmetry of the geometry and boundary conditions, the domain has been assumed axisymmetric. For this situation, boundary and initial conditions in non-dimensional form have been defined as follows:

Initial conditions:

$$\vec{v}^* = 0, \quad \Theta = \Theta_0 \tag{7}$$

At the cylinder axis:

$$v_r^* = 0, \qquad \frac{\partial v_z^*}{\partial r^*} = 0, \qquad \frac{\partial \Theta}{\partial r^*} = 0 \tag{8}$$

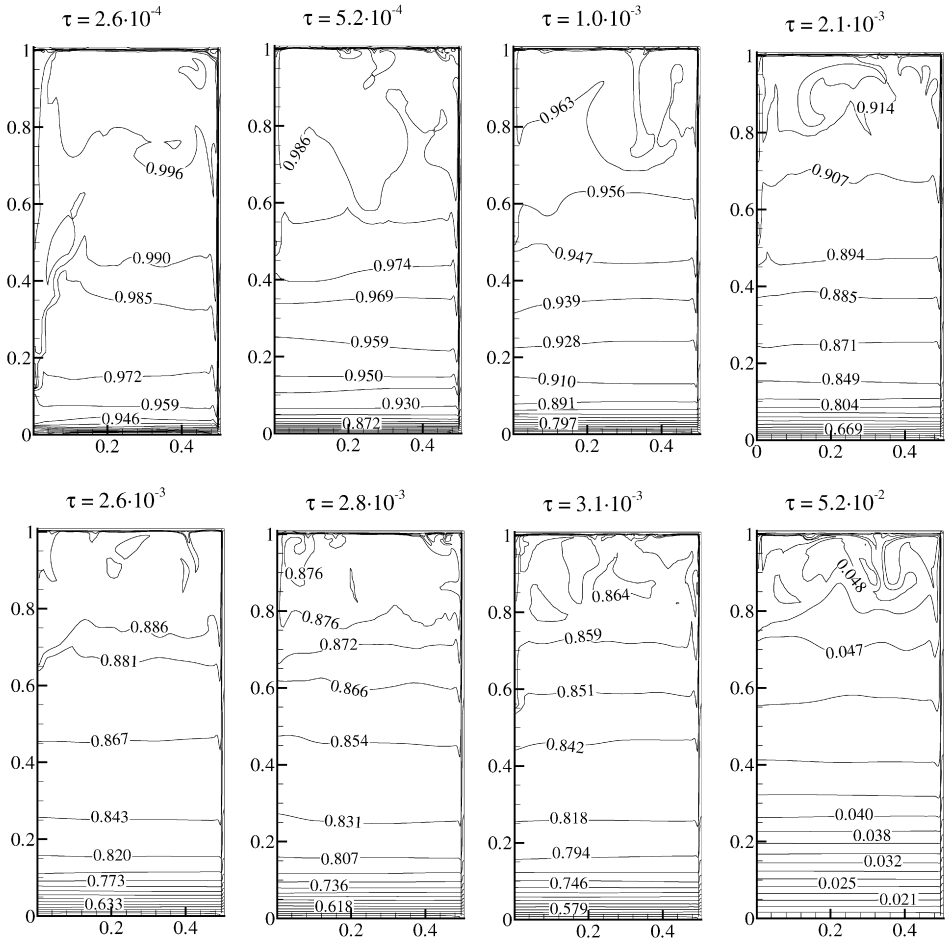

Fig. 5. Transient evolution of the fluid inside the tank. Temperature contours. $\tau = 2.6 \cdot 10^{-4}$ to $\tau = 5.2 \cdot 10^{-2}$. $Ra = 5.986 \cdot 10^{11}$, $H/D = 1$, and $U^* = 11.6$.

At the lateral wall:

$$-\frac{\partial \Theta}{\partial r^*} = \frac{h_{\text{ext}} H}{k_{\text{ins}}} \Theta \tag{9}$$

At the top and bottom walls:

$$-\frac{\partial \Theta}{\partial z^*} = \frac{h_{\text{ext}} H}{k_{\text{ins}}} \Theta \tag{10}$$

With the aim of identifying the relevant non-dimensional groups that govern the behaviour of the fluid, boundary conditions for the fluid are defined as:

At the lateral walls:

$$\vec{v}^* = 0\,, \; -\frac{\partial \Theta}{\partial r^*} = \frac{\overline{U} H}{k}\left(\Theta + \frac{1}{2}\right) \tag{11}$$

At the top and bottom walls:

$$\vec{v}^* = 0\,, \; -\frac{\partial \Theta}{\partial z^*} = \frac{\overline{U} H}{k}\left(\Theta + \frac{1}{2}\right) \tag{12}$$

In the above formulation, it has been assumed that the heat transfer through the walls and insulation material is one-dimensional and normal to the wall surfaces. Furthermore, considering the situations described in Section 2, it can also be assumed that these coefficients are nearly the same on the top, bottom and lateral walls (i.e. $\overline{U}_B \simeq \overline{U}_T \simeq \overline{U}_H \simeq U$). From the boundary conditions for the fluid, two non-dimensional groups appear: the aspect ratio (H/D) and a dimensionless group referred to the overall heat transfer coefficient ($\widehat{U} = \overline{U} H/k$). Thus, considering governing equations and boundary conditions for the problem analysed, the fluid temperature inside the store depends on the following non-dimensional groups:

$$\Theta = f(\vec{r}^*, \tau, Ra, \widehat{U}, H/D, Pr) \tag{13}$$

On the other hand, the dimensionless heat transfer coefficient, i.e. the Nusselt number, can be defined as:

$$\overline{Nu} = \frac{\overline{h} H}{k} = \frac{1}{(\overline{\Theta} - \overline{\Theta}_w) S} \int_{\partial \Omega} \left(\frac{\partial \Theta}{\partial n}\right) dS \tag{14}$$

The Nusselt number is a function of the non-dimensional fluid and wall temperatures. Thus, considering the dependence of the temperature with the relevant non-dimensional groups identified, in a general sense, the Nusselt number can be expressed as a function of those parameters as:

$$\overline{Nu} = f(\tau, Ra, \widehat{U}, H/D, Pr) \tag{15}$$

4.2. Parametric study

In order to find the relation between the Nusselt number with the relevant non-dimensional groups that characterise the un-

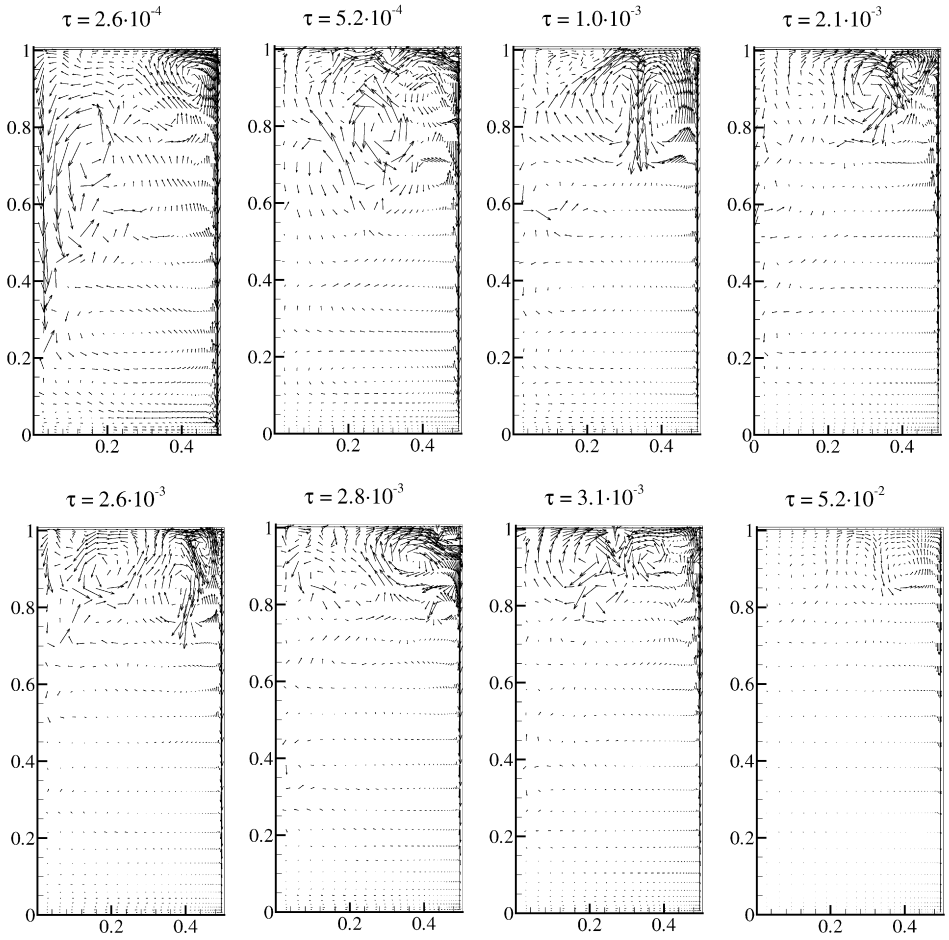

Fig. 6. Transient evolution of the fluid inside the storage tank. Velocity vectors. $\tau = 2.6 \cdot 10^{-4}$ to $\tau = 5.2 \cdot 10^{-2}$. $Ra = 5.986 \cdot 10^{11}$, $H/D = 1$, and $U^* = 11.6$.

steady natural convection inside the tank, a parametric study has been carried out by means of the resolution of detailed numerical simulations.

The study has accounted for the variation of the different relevant non-dimensional groups, i.e. Ra, H/D, $\widehat{U}$. As governing equations (Eqs. (1)–(3)) have been solved in dimensional form, these parameters have been defined from the dimensional problem parameters (the insulation thickness δ_{ins}, the initial fluid temperature T_0, the ambient temperature T_{env}, the tank volume Ω, etc.). Therefore, values for each parameter have been considered within the ranges defined in Section 2. Four different values for the aspect ratio $H/D = 1, 2, 3, 3.45$; six values for the initial temperature $T_0 = 40, 50, 55, 60, 65, 70\,^{\circ}\text{C}$; four for the insulation thickness $\delta_{\text{ins}} = 0, 0.01, 0.02, 0.04$ m; four for the tank volume $\Omega = 0.1, 0.2, 0.3, 0.4$ m^3 and two for the external heat transfer coefficient $h_{\text{ext}} = 2, 10$ W/m^2 K have been used. Ambient temperature in all situations has been set to $T_{\text{env}} = 20\,^{\circ}\text{C}$. These account for $4.8 \cdot 10^{11} \leqslant Ra \leqslant 10^{13}$, $1 \leqslant H/D \leqslant 3.45$ and $0.78 \leqslant \widehat{U} \leqslant 26.6$.

Taking into account that the total amount of cases considered for the parametric study equals 768, and that in terms of computational effort the resolution of the transient cooling process of all cases could be very costly, a further selection has been performed. First, for a fixed tank volume $\Omega = 0.3$ m^3 and initial temperature $T_0 = 60\,^{\circ}\text{C}$, all other situations have been considered (i.e. a total of 32 cases considering four aspect ratios, four insulation thickness and two external heat transfer). After that, for the aspect ratio of $H/D = 3.45$, initial temperature of $T_0 = 60\,^{\circ}\text{C}$ and insulation thickness of $\delta_{\text{ins}} = 0.01$ m, four tank volumes have been considered. Thus, fixing the insulation thickness to $\delta_{\text{ins}} = 0.02$ m, the tank volume $\Omega = 0.3$ m^3 and the external heat transfer coefficient $h_{\text{ext}} = 10$ W/m^2 K, seven initial temperatures have been investigated. These have resulted in a total number of 42 situations for the transient numerical simulation of the cooling process of the tank.

4.3. Development of correlations

4.4. The average heat transfer coefficient

According to the non-dimensional analysis carried out in Section 4.1, the Nusselt number (Nu) can be expressed in terms of the non-dimensional groups τ, Ra, H/D, $\widehat{U}$ and Pr. In the present work, as the working fluid is water, the dependence with the Prandtl number (Pr) in the studied range of relevant parameters has been implicitly considered. This treatment can be assumed because in the working range studied, the fluid properties vary slightly with the temperature, being these variations within the Rayleigh number ($Ra = Gr \cdot Pr$). There are some works in the literature that validate this treatment [5,13]. The

first [5], studied the unsteady convection of a flow inside a rectangular cavity for different *Ra* and *Pr* numbers, concluding that for steady situations *Nu* proved to be independent of *Pr* number. The latter [13], studied the influence of *Pr* number among other parameters on the cooling process of a fluid in a cylindrical enclosure after a step change in the vertical and bottom walls temperature. In their study, they considered a range of $1 \leqslant Pr \leqslant 1000$, finding no dependence of the transient temperature and the *Nu* number on *Pr* for the sidewall, while no significant influence of this parameter on *Nu* at the bottom wall was found. They also concluded that, despite this weak *Pr* dependence on the bottom wall, the overall heat transfer rate (bottom plus sidewalls) is not affected by this dependence, as the cooling process is dominated by sidewall heat transfer. However, the validity of this treatment for the range of parameters considered in the present study, i.e. neglect the influence of the *Pr* number on the mean Nusselt number $\overline{Nu}$, is commented further.

Taking into account the aforementioned hypothesis and the non-dimensional analysis done, the following dependence for $\overline{Nu}$ with the relevant parameters identified has been proposed:

$$\overline{Nu} = C_1 \tau^{C_2} Ra^{C_3} \widehat{U}^{C_4} (H/D)^{C_5} \tag{16}$$

The data set from the several computations carried out has been fitted to the above scaling relation proposed for the Nusselt number. In order to find the values of the constants, the fitting process of all data has been performed by means of the *GNU Regression, Econometrics and Time-series Library (gretl)* [23]. This library offers a full range of least-squares based estimators, including two-stage least squares and nonlinear least squares data fit, among other possibilities. The actual fitting process has been carried out using the Levenberg–Marquardt algorithm [24] implemented in this library. This method provides the solution to the non-linear function, minimising the sum of the squares of the deviations. From the curve-fitting, the constants in Eq. (16) have arisen:

$$\overline{Nu} = 4.5851 \tau^{-0.1686} Ra^{0.0686} (H/D)^{0.5304} \widehat{U}^{0.1981} \tag{17}$$

Scaling relation (17) has shown a good agreement with all the data set, as can be observed in Fig. 7(a), with a goodness of the fit of $R^2 = 0.994$ and a standard deviation of the residuals of 5.171. In the figure, data from numerical results and the correlated ones have been arranged in order to plot the data as a function of the non-dimensional time (τ). In Fig. 7(b), the relative errors between the fitted data and results from the correlation are also shown. The maximum relative error has been found below 12%, and the average relative error in the order of 2.7%. Major discrepancies have been obtained for large values of the non-dimensional time. These values correspond to the cases with the largest cooling time (lowest H/D and highest $\widehat{U}$), which are in the limits of the studied range, and the number of samples to be correlated were only a few.

Fig. 8 shows the data obtained from the detailed numerical simulations as a function of the non-dimensional time for different *Pr* in the range of study. The data has been arranged by using the scaling relations for *Ra*, $\widehat{U}$ and H/D non-dimensional numbers. As can be observed, there is no dependence of the mean $\overline{Nu}$ number on *Pr*. The six curves corresponding to each

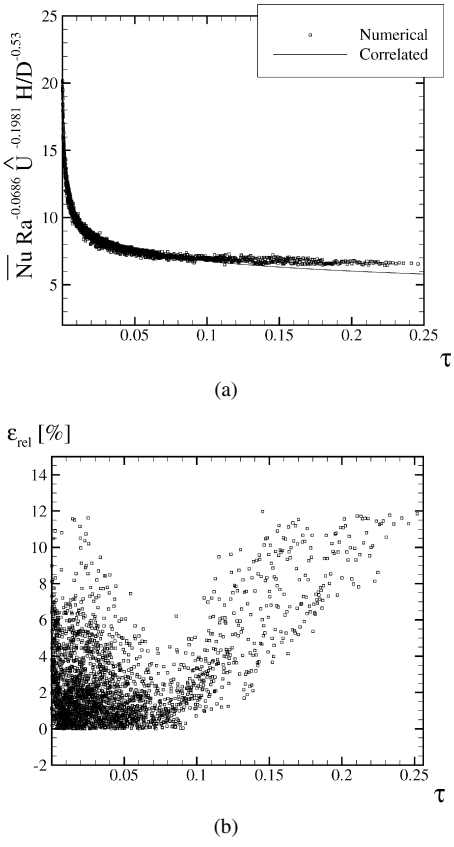

Fig. 7. Results from the curve fitting. Nusselt number. (a) Comparison between fitted data and correlated one. (b) Relative errors between raw data and correlated results with Eq. (17).

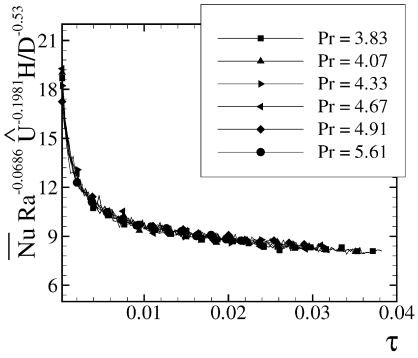

Fig. 8. Results of the curve fitting. Influence of the *Pr* number in the average Nusselt number, $\overline{Nu}$.

Pr considered collapse into the same curve. Taking into account these results, the hypothesis of neglecting the influence of *Pr* on the Nusselt number can be assumed, at least within the range $3.83 \leqslant Pr \leqslant 5.61$.

4.5. The transient temperature distribution

Alternatively to the resolution of the differential equation for the global balance (Eq. (22)), in the present analysis the mean fluid temperature has been approximated to the following relation:

$$\overline{\Theta} = \exp\left(C_6 \tau Ra^{C_7} \widehat{U}^{C_8} (H/D)^{C_9}\right) \tag{18}$$

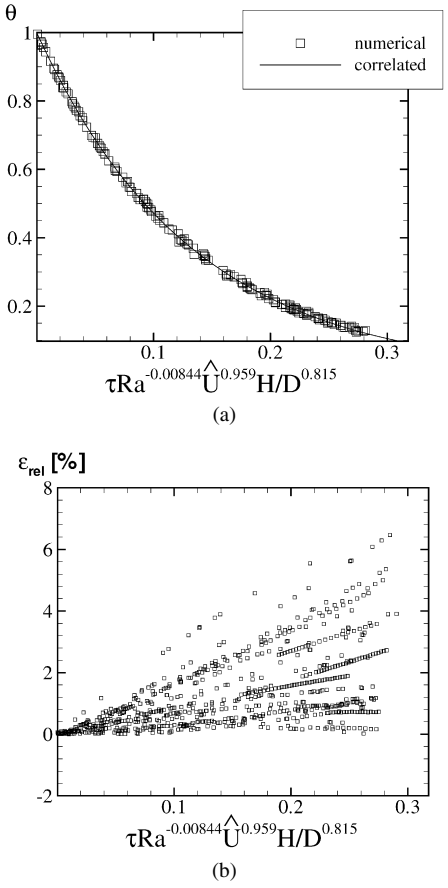

Fig. 9. Non-dimensional transient mean fluid temperature. (a) Comparison between numerical and correlated results. (b) Relative errors between raw data and Eq. (19).

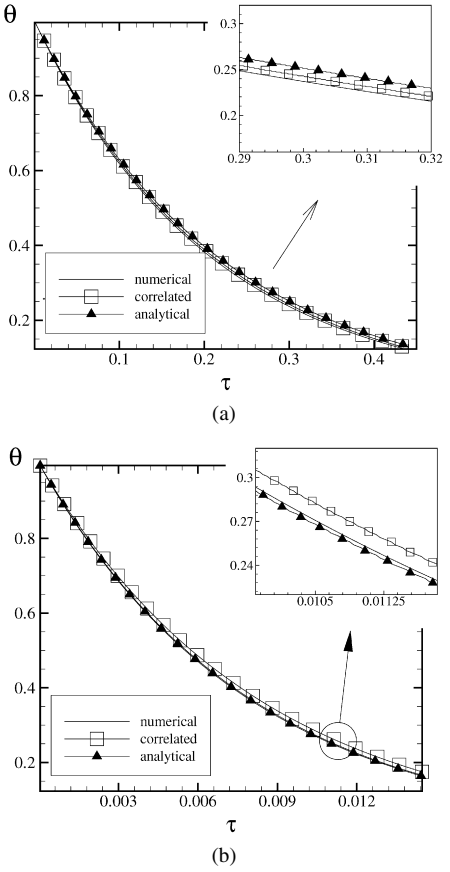

Fig. 10. Comparison with numerical results for two illustrative cases: (a) $Ra = 2.36 \cdot 10^{12}$, $\widehat{U} = 1.274$ and $(H/D) = 2$; (b) $Ra = 9.5 \cdot 10^{12}$, $\widehat{U} = 8.224$ and $(H/D) = 3.45$.

Following the same procedure as for the average Nusselt number, the mean fluid temperature inside the tank obtained from the numerical simulations has been adjusted. Results of the curve fitting gives:

$$\overline{\Theta} = \exp\left(-7.506\tau Ra^{-0.0084} H/D^{0.8150} \widehat{U}^{0.9587}\right) \tag{19}$$

In Fig. 9(a), the raw data with results of the correlation (19) are compared, while in Fig. 9(b) the relative error between numerical results and values from the correlation are plotted. As can be observed in both figures, all data correlates quite well, with a goodness of the fit of $R^2 = 0.9996$ and a standard deviation of the residuals of 0.00449. The maximum relative error obtained has been less than 6.8%, and the mean relative error around 1.23%.

5. Global thermodynamic model

The aim of the study is to characterise the transient behaviour of the fluid inside the storage tank, evaluating the long-term variation of its mean temperature and the heat losses to the environment. According to this objective, and considering the problem defined, a simplified mathematical model is hereafter explained.

5.1. Basic mathematical formulation

For the model, the fluid inside the tank is at a mean temperature $\overline{T}$; thermophysical properties are constant, evaluated at the average temperature between the initial temperature of the fluid and the ambient; heat losses have been modelled by an overall heat transfer coefficient between the inner walls and the ambient ($\overline{U}$) and; the energy storage capacity of the solid walls has been neglected. Under these conditions, the transient evolution of the mean fluid temperature can be evaluated as:

$$\rho c_p \frac{\partial \overline{T}}{\partial t} \Omega = -\int_{\partial\Omega} \vec{q} \cdot d\vec{S} = -\dot{Q}_{\text{loss}} \tag{20}$$

Eq. (20) expresses that the transient variation of the mean temperature of the fluid equals the energy losses through the top, bottom and lateral walls expressed by $\dot{Q}_{\text{loss}}$. The heat losses through the walls can be evaluated as:

$$\dot{Q}_{\text{loss}} = \bar{h}(\overline{T} - \overline{T}_w)S = \overline{U}(\overline{T}_w - T_{\text{env}})S \tag{21}$$

Thus, Eq. (20) reads:

$$\rho c_p \frac{\partial \bar{T}}{\partial t} \Omega = -\left(\frac{\overline{U}\bar{h}S}{\overline{U} + \bar{h}}\right)(\overline{T} - T_{\text{env}}) \tag{22}$$

The global model represented by Eq. (22) can be easily integrated mathematically or numerically. The main problem of

these kinds of global models is the lack of empirical data (or correlations) of the transient heat transfer coefficient to feed them properly. Hereafter, the correlation for the Nusselt number obtained in previous section has been used to feed-back the global model.

5.2. Resolution methodology

As has been commented, the objective of the analysis is twofold: to characterise the cooling process of the fluid and to predict the behaviour of the mean fluid temperature and the heat losses to the environment. The resolution of both, the temperature and the heat losses, is summarised by means of the application of the thermodynamic global model represented by Eq. (22). From the model, it is possible to evaluate the transient evolution of the mean fluid temperature in the storage tank, by using the correlation proposed in previous section for the transient $\overline{Nu}$ (Eq. (17)). Thus, the heat transfer coefficient at any instant can be evaluated as:

$$\bar{h} = \frac{\overline{Nu}k}{H} = 4.58\tau^{-0.1685} Ra^{0.0686} (H/D)^{0.53} \widehat{U}^{0.1981} \frac{k}{H} \tag{23}$$

The above expression can also be written in a general form as:

$$\bar{h} = \Pi t^n \tag{24}$$

where

$$\Pi = 4.58 Ra^{0.0686} (H/D)^{0.53} \widehat{U}^{0.1981} \frac{k\alpha^{-0.1685}}{H^{0.663}} \tag{25}$$

$$n = -0.1685 \tag{26}$$

Substituting Eq. (24) in the global balance (Eq. (22)), the transient mean fluid temperature can be calculated as:

$$\frac{d\overline{T}}{dt} = -\frac{1}{\rho c_p \Omega} \frac{\overline{U}\Pi t^n}{\overline{U} + \Pi t^n} (\overline{T} - T_{\text{env}}) S \tag{27}$$

The differential equation (27) can be integrated for the initial conditions ($t = 0$, $\overline{T} = T_0$) giving:

$$\overline{T} = T_{\text{env}} + (T_0 - T_{\text{env}}) \exp\left(- \int_{t=0}^{t} \frac{S}{\rho c_p \Omega} \frac{\overline{U}\Pi t^n}{\overline{U} + \Pi t^n} dt \right) \tag{28}$$

The analytical solution of the integral term in Eq. (28) gives as a result the first hypergeometric function which its regular solution involves an infinite series expansion in factorial notation [25]. Thus, in order to obtain the transient evolution of the temperature of the fluid, a numerical integration of the above equation could be computationally less expensive. This can be done by approximating the integral term as a summation, giving:

$$\overline{T} = T_{\text{env}} + (T_0 - T_{\text{env}}) \exp\left(- \sum_{k=1}^{N} \frac{S}{\rho c_p \Omega} \frac{\overline{U}\Pi t_k^n}{\overline{U} + \Pi t_k^n} \Delta t \right) \tag{29}$$

where

$$t_k = \frac{\Delta t}{2} + (k-1)\Delta t \quad \text{and} \quad N = \frac{t}{\Delta t} \tag{30}$$

The results obtained by means of the numerical integration of Eq. (29), and the correlation proposed for the mean temperature (Eq. (19)), have been compared with the data from numerical simulations (see Fig. 10 (a) and (b)). Cases plotted in both figures have been selected as illustrative results. These cases correspond to: $Ra = 2.36 \cdot 10^{12}$, $\widehat{U} = 1.274$ and $(H/D) = 2$ for Fig. 10(a) and to $Ra = 9.5 \cdot 10^{12}$, $\widehat{U} = 8.224$ and $(H/D) = 3.45$ for Fig. 10(b). The numerical integration of Eq. (29) has been carried out by using time steps of $\Delta t = 100$ s. Smaller time steps have also been tested, but differences between results were not significant. As can be observed, the mean temperature evaluated from Eq. (29) and the correlation (19) agree quite well with numerical results. Maximum differences have been obtained at the final instants of the cooling process, where $\overline{Nu}$ correlation obtained gives the highest discrepancies.

Once the temperature evolution is known, the heat losses of the fluid from the initial instant ($t = 0$) to any time of the cooling process can be evaluated as:

$$\dot{Q}^{\text{loss}}_{t=0\to t} = c_p (T_0 - T_{\text{env}}) \times \left[1 - \exp\left(- \int_{t=0}^{t} \frac{S}{\rho c_p \Omega} \frac{\overline{U}\Pi t^n}{\overline{U} + \Pi t^n} dt \right) \right] \rho\Omega \tag{31}$$

where the integral term is approximated numerically as:

$$\dot{Q}^{\text{loss}}_{t=0\to t} = c_p (T_0 - T_{\text{env}}) \times \left[1 - \exp\left(- \sum_{k=1}^{N} \frac{S}{\rho c_p \Omega} \frac{\overline{U}\Pi t_k^n}{\overline{U} + \Pi t_k^n} dt \right) \right] \rho\Omega \tag{32}$$

where t_k and N are evaluated as in Eq. (30).

The methodology for the evaluation of the cooling process of a fluid under heat losses to the ambient by means of the global model is summarised as follows:

(1) Define the case and evaluate the relevant parameters Ra, $\widehat{U}$ and H/D.
(2) Evaluate the value of the constant Π by means of Eq. (25).
(3) Solve numerically Eq. (29) from $t = 0$ to any instant t of the cooling process and obtain the mean temperature.
(4) Evaluate heat losses through the tank walls from $t = 0$ to any instant t of the cooling process, by solving numerically Eq. (32).

In order to evaluate heat losses at any instant:

(1) Evaluate mean Nusselt number from Eq. (17) at the time of interest.
(2) Evaluate the superficial heat transfer coefficient by

$$\bar{h} = \overline{Nu} \frac{k}{H} \tag{33}$$

(3) Solve numerically Eq. (29) from $t = 0$ to any instant t of the cooling process and obtain the mean temperature.
(4) Evaluate instantaneous heat losses to the ambient as:

$$\dot{Q}_{\text{loss}} = \frac{\overline{U}\bar{h}}{\overline{U} + \bar{h}} (\overline{T} - T_{\text{env}}) S \tag{34}$$

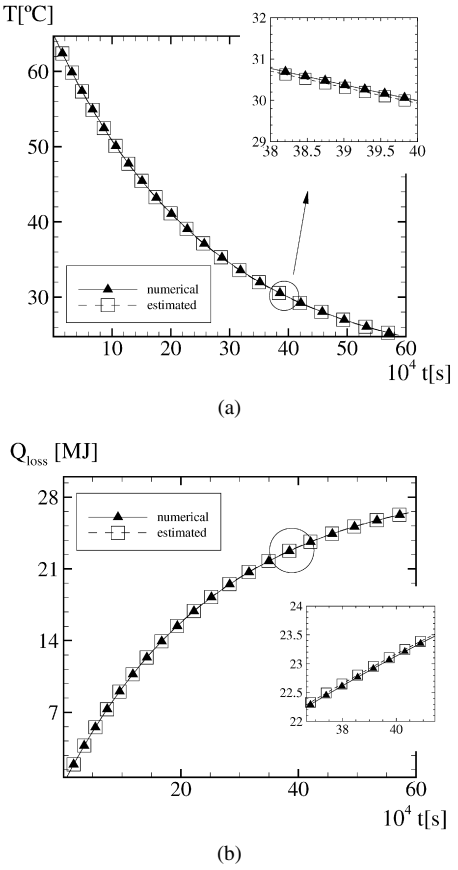

Fig. 11. Comparison between numerical experiments and results from the global model. $H/D = 2.77$; $Ra = 2.87 \cdot 10^{12}$; $\widehat{U} = 2.59$. (a) Mean transient temperature. (b) Cumulative heat losses.

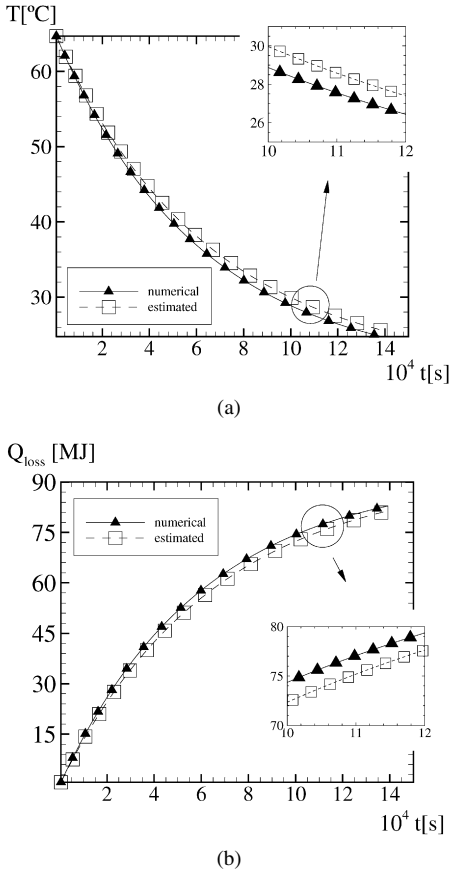

Fig. 12. Comparison between numerical experiments and results from the global model. $H/D = 2.05$; $Ra = 4.9 \cdot 10^{12}$; $\widehat{U} = 20.12$. (a) Mean transient temperature. (b) Cumulative heat losses.

5.3. Verification of the global thermodynamic model

With the objective of verifying the scaling relations obtained in the working range studied, a new set of cases has been selected. This new set of cases accounted for tank volumes of: $\Omega = 0.16$, 0.3 and 0.5 [m^3], with aspect ratios of: $H/D = 2.05$, 2.77 and 3.2. The insulation of the tank has been set to $\delta_{ins} = 0$ and 2.5 cm. For these cases, initial temperature of $T_0 = 65\,^{\circ}C$ and external heat loss coefficient of $h_{ext} = 10$ W/m^2 K have been imposed. Ambient temperature and properties of the insulation material have also been varied. Ambient temperatures considered have been of $T_{env} = 15$ and 20 °C, while polyurethane insulation material has also been considered. All the selected cases were within the range studied for the relevant parameters (Ra, $\widehat{U}$, H/D) except one, which exceeded slightly the maximum Ra number considered in the correlations.

In Figs. 11 and 12 some of the results obtained with the set of cases are shown. In the figures, the cumulative heat losses through the tank walls and the mean fluid temperature estimated are compared with the results of the numerical simulations. For all cases, maximum and relative errors for the mean temperature and cumulative heat losses predicted by the global model have been computed. A good prediction of both quantities has been obtained. Major discrepancies have been obtained for the cases with the highest non-dimensional overall heat transfer coefficient. In these situations, maximum error for the cumulative heat losses and temperature have been of 10 and 3.8%, respectively, while the mean relative errors have been of 3.9 and 2.8%. In most of the cases tested, the maximum error obtained has been below 5% for the cumulative heat losses.

From this analysis, it can be observed that the proposed methodology, together with the correlations for the mean fluid temperature and Nusselt number, have a good behaviour within the range of the relevant parameters studied. The predicted results have been shown to be within an acceptable error tolerance considering the limitations of these global models. All the cases studied have been in the range of application for domestic hot water storage tanks. Although this is a wide range, the use of these correlations outside the limits considered could fail. In order to extrapolate the current results beyond this range, further studies would be necessary.

6. Conclusions

The transient process of cooling-down a fluid initially at rest by heat transfer through the walls and insulation material has been investigated numerically.

In order to describe the long-term behaviour of the fluid inside the storage tank, a global prediction model has been proposed. In the model, the transient behaviour of the fluid has been represented by the mean fluid temperature and the global

heat losses through the walls. In order to characterise these heat losses, a non-dimensional analysis has been carried out. This analysis has led to the identification of the significant parameters that define the transient natural convection phenomena inside the storage: the Rayleigh number Ra, the aspect ratio H/D, and the non-dimensional overall heat loss coefficient imposed by the boundary conditions of the problem under study. Negligible influence of the Prandtl number variations (Pr), has been observed within the range considered.

A parametric study consisting of 42 different transient situations has been performed with the aim of finding the correlation that describes the transient behaviour of the Nusselt number. Variations on the different relevant parameters have been taken into account. The situations considered in the study have been within the working range for domestic hot water applications. The average Nusselt number at each instant of all numerical simulations, have been fitted to a scaling relation proposed in terms of the identified relevant parameters. The non-dimensional heat transfer coefficient ($\overline{Nu}$) is well represented by the correlation obtained, being maximum relative errors below 12%.

It has been shown that the global thermodynamic model together with the non-dimensional heat transfer coefficient correlation proposed is capable of quantify the heat losses to the ambient and predict the transient behaviour of the fluid temperature inside the tank, being in good agreement with numerical results obtained. This model provides a mean of evaluating and predict the transient cooling process of the fluid, with low computational effort and an accuracy within the limits of this kind of simplified model approach. However, correlations such as those developed should be applied with due regard outside the range of significant parameters on which they rest.

Acknowledgements

This work has been financially supported by "Comisión Interministerial de Ciencia y Tecnologia", Spain (project TIC-2003-0790).

References

[1] G. De Vahl Davis, Natural convection of air in a square cavity: A benchmark numerical solution, International Journal for Numerical Methods in Fluids 3 (1983) 249–264.

[2] G. Mallison, G. De Vahl Davis, Three-dimensional natural convection in a box: a numerical study, Journal of Fluid Mechanics 83 (1977) 1–31.

[3] J. Vierendeels, B. Merci, E. Dick, Numerical study of convective heat transfer with large temperature differences, International Journal of Numerical Methods in Heat and Fluid Flow 11 (4) (2001) 329–341.

[4] M.A. Sharif, T.R. Mohammad, Natural convection in cavities with constant flux heating at the bottom wall and isothermal cooling from the sidewalls, International Journal of Thermal Science 44 (2005) 865–878.

[5] J. Patterson, J. Imberger, Unsteady natural convection in a rectangular cavity, Journal of Fluids Mechanics 100 (1980) 65–86.

[6] V. Nicolette, K. Yang, J. Lloyd, Transient cooling by natural convection in a two dimensional square enclosure, International Journal of Heat and Mass Transfer 28 (9) (1985) 1721–1732.

[7] I. Kurtbaç, A. Durmuç, Unsteady heat transfer by natural convection in the cavity of a passive heating room, International Journal of Thermal Sciences 47 (8) (2008) 1026–1042.

[8] J. Hyun, Transfer process of thermally stratifying an initially homogeneous fluid in an enclosure, International Journal of Heat and Mass Transfer 27 (10) (1984) 1936–1938.

[9] W. Rosehnow, J. Hartnett, E. Ganić (Eds.), Handbook of Heat Transfer Fundamentals, McGraw-Hill Book Company, 1985, pp. 6-67–6-68 (Ch. Natural Convection).

[10] M. Cotter, M. Charles, Transient cooling of petroleum by natural convection in cylindrical storage tanks. I. Development and testing the numerical simulator, International Journal of Heat and Mass Transfer 36 (8) (1993) 2165–2174.

[11] M. Cotter, M. Charles, Transient cooling of petroleum by natural convection in cylindrical storage tanks. II. Effect of heat transfer coefficient, aspect ratio and temperature-dependent viscosity, International Journal of Heat and Mass Transfer 36 (8) (1993) 2175–2182.

[12] W. Lin, S. Armfield, Direct simulation of natural convection cooling in a vertical circular cylinder, International Journal of Heat and Mass Transfer 42 (1999) 4117–4130.

[13] W. Lin, S. Armfield, Long-term behaviour of cooling fluid in a vertical cylinder, International Journal of Heat and Mass Transfer 48 (2005) 53–66.

[14] R.D.C. Oliveski, A. Krezinger, H. Vielmo, Cooling of cylindrical vertical tanks submitted to natural internal convection, International Journal of Heat and Mass Transfer 46 (2003) 2015–2026.

[15] E. Papanicolaou, V. Belessiotis, Transient natural convection in a cylindrical enclosure at high Rayleigh numbers, International Journal of Heat and Mass Transfer 45 (2002) 1425–1444.

[16] F. Fernández-Seara, J. Uhía, J. Sieres, Experimental analysis of a domestic electric hot water storage tank. Part I: Static mode of operation, Applied Thermal Engineering 27 (1) (2007) 129–136.

[17] P. Gaskell, A. Lau, Curvature-compensated convective transport: SMART, a new boundedness-preserving transport algorithm, International Journal for Numerical Methods in Fluids 8 (1988) 617–641.

[18] J. Van Doormal, G. Raithby, Enhancements of the simple method for predicting incompressible fluid flows, Numerical Heat Transfer 7 (1984) 147–163.

[19] B. Hutchinson, G. Raithby, A multigrid method based on the additive correction strategy, Numerical Heat Transfer, Part B 9 (1986) 511–537.

[20] K. Salari, P. Knupp, Code verification by the method of manufactured solutions, Tech. rep., Sandia National Laboratories, 2000.

[21] I. Rodríguez, Unsteady laminar convection in cylindrical domains: numerical studies and application to solar water storage tanks, Ph.D. thesis, Universitat Politècnica de Catalunya, 2006.

[22] J. Cadafalch, C. Pérez-Segarra, R. Còsul, A. Oliva, Verification of finite volume computations on steady state fluid flow and heat transfer, Journal of Fluids Engineering 124 (2002) 11–21.

[23] A. Cottrell, R. Lucchetti, Gretl, GNU Regression, Econometrics and Time-series Library, version 1.5.0, 2005.

[24] D. Marquardt, An algorithm for least-squares estimation of nonlinear parameters, SIAM Journal of Applied Mathematics 11 (1963) 431–441.

[25] M. Abramowitz, I. Stegun (Eds.), Handbook of Mathematical Functions with Formulas, Graphs and, Mathematical Tables, ninth ed., Dover, New York, 1972, pp. 555–566 (Ch. 15, Hypergeometric functions).